ChemPubSoc Europe

DOI: 10.1002/open.201900291

Open Access ChemistryOPEN Full Paper

Special Collection

Self-Assembly of Bowl-Shaped Naphthalimide-Annulated Corannulene

Rebecca Renner, Matthias Stolte, and Frank Würthner*[a]

Dedicated to Professor Jean-Marie Lehn on the occasion of his 80th birthday

The self-assembly of a bowl-shaped naphthalimide-annulated corannulene of high solubility has been studied in a variety of solvents by NMR and UV/Vis spectroscopy. Evaluation by the anti-cooperative K_2-K model revealed the formation of supramolecular dimers of outstanding thermodynamic stability. Further structural proof for the almost exclusive formation of dimers over extended aggregates is demonstrated by atomic force microscopy (AFM) and diffusion ordered spectroscopy (DOSY) measurements as well as by theoretical calculations. Thus, herein we present the first report of a supramolecular dimer of an annulated corannulene derivative in solution and discuss its extraordinarily high thermodynamic stability with association constants up to $>10^6\ M^{-1}$ in methylcyclohexane, which is comparable to the association constants given for planar phthalocyanine and perylene bisimide dyes.

1. Introduction

Corannulene, a non-planar polycyclic aromatic hydrocarbon (PAH), has recently attracted significant attention. Due to its bowl-shaped structure it exhibits a moderate ground state dipole moment ($\mu_g = 2.1$ D)[1] and enhanced solubility in common organic solvents[2] compared to planar PAHs. Other bowl-shaped molecules like subphthalocyanines[3–4] and sumanenes[5] also exhibit these properties, due to the two different faces of the molecules. By functionalization of the rim, the bowl depth and thus the packing in the solid state as well as in solution can be controlled, making these non-planar systems interesting candidates for application in supramolecular host-guest chemistry to obtain complex functional structures.[6–8] Furthermore, corannulene was shown to be a useful precursor for the synthesis of large non-planar nanographenes by annulative π-extension to give new, structurally alluring molecular shapes and motifs.[9–11]

Bowl-shaped molecules are widely applied in the field of supramolecular chemistry as hosts for fullerene molecules after Scott and coworkers first showed the assembly of C_{60} with corannulene in the solid state[12] and in solution[13] due to the complementary intimate concave-convex π-π-interactions. By connecting two bowl-shaped precursors with a rigid bridge, it was further possible to synthesize the "buckycatcher", a molecular tweezer which is able to form a supramolecular 1:1 complex with C_{60} through concave-convex π-π-interactions.[14] Different types of buckycatchers have been synthesized and investigated accordingly to exploit this unique feature in search of selectivity in the binding of different fullerene derivatives.[15–16]

An important property to be considered in the supramolecular self-assembly of bowl-shaped molecules is the bowl-to-bowl inversion. This effect is commonly observed for corannulene systems, due to the relative low lying barrier for the bowl inversion, depending on the substituents. Usually, the activation barrier in sumanene systems is higher and subphthalocyanines usually do not undergo bowl inversion at all due to very high barriers.[17] Conformationally stable systems, in which the bowl-to-bowl inversion is hindered, can be aligned in the presence of an electric field to form one-dimensional columnar liquid crystalline materials due to their axial dipole moment, which is of interest for device applications.[18] Upon chemical reduction of corannulene and sumanene, highly negatively charged bowl-shaped ligands are obtained, forming a variety of intriguing sandwich-like complexes with different alkali metal cations on both the convex and the concave surface of the ligand, which have been characterized in their crystalline state and by NMR spectroscopy.[19–20]

By introducing electron-withdrawing substituents e.g. halogens or nitrile groups on the rim of the corannulene system the electronic properties of the molecules can be altered which is of interest for their use in organic electronics as n-type semiconductors.[21-23] The same attributes can be achieved via extension of the aromatic π-system with naphthalimide moieties using a Suzuki-Miyaura cross coupling/Heck type arylation cascade annulation reaction to establish an interesting new class of bowl-shaped PAHs.[24] These new molecules exhibit intriguing optical and electronic properties, being among the highest fluorescent π-conjugated bowl-shaped dyes. Their low-lying frontier orbitals offer the possibility to use them in

[a] R. Renner, Dr. M. Stolte, Prof. Dr. F. Würthner
Institut für Organische Chemie & Center for Nanosystems Chemistry, Universität Würzburg
Am Hubland, 97074 Würzburg (Germany)
E-mail: wuerthner@uni-wuerzburg.de

Supporting information for this article is available on the WWW under https://doi.org/10.1002/open.201900291

Special Collection *An invited contribution to a Special Collection dedicated to Functional Supramolecular Systems*

supramolecular photosystems and as n-type semiconductors, making them promising candidates for bulk-heterojunction solar cells.

In this work, we explore the self-assembly of a new, highly soluble derivative of our recently reported first bowl-shaped bis-naphthalimide-annulated corannulene.[24] Our previously described molecule containing diisopropylphenyl units at the imide position was not able to self-assemble in solution within the available concentration range due to the bulky isopropyl substituents. Thus, the new derivative **3a** was synthesized with solubilizing tridodecylphenyl side chains. Here we will show that **3a** forms supramolecular dimers of outstanding thermodynamic stability in various solvents. To the best of our knowledge, we herein explore the thermodynamics of self-assembly for a corannulene derivative for the first time. The applied techniques for structural elucidation, AFM and DOSY, reveal the formation of dimers. Theoretical calculations were conducted to propose two possible structures for the dimer, one based on the maximization of the π-π-interactions between two molecules and the other based on dipolar interactions.

2. Results and Discussion

2.1. Synthesis

The synthesis of **3a** could be achieved by altering a literature known route for Suzuki-Miyaura coupling and direct arylation, as it was not possible to synthesize the product using the literature known procedure in sufficient yield and purity (Scheme 1).[25] Using tri(*m*-tolyl)phosphine instead of tricyclohexylphosphine tetrafluoroborate as ligand in the reaction, the product **3a** was isolated as a dark red solid in a yield of 28%. The new molecule as well as the precursor **2a** were characterized using ^{1}H and ^{13}C NMR spectroscopy (Figure S1–S4) and mass spectrometry (MALDI, DIP, ESI). The literature known molecule **3b** could also be synthesized under these new conditions in a yield of 24%.

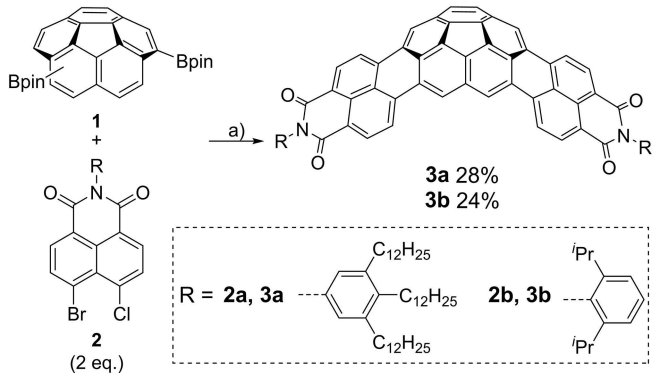

Scheme 1. Synthesis of bowl-shaped polycyclic aromatic bis(dicarboximides) **3a** and **3b**. a) $[Pd_2(dba)_3]\cdot CHCl_3$ (5 mol%), P(*m*-tolyl)$_3$ (20 mol%), Cs_2CO_3 (6 equiv.), 1-chloronaphthalene; Bpin: boron(pinacol)ester.

2.2. Optical Properties

The optical properties of the new corannulene derivative **3a** were firstly investigated in dichloromethane (DCM, Figure 1) and compared with the previously reported molecule **3b**.

In this highly polarizable solvent, the band shape as well as the absorption maximum of the S_0–S_1 transition, that appears at $\lambda_{max} = 536$ nm, are in good accordance with the reported absorption spectrum, which is typical for this type of corannulene deriative, and wavelength for the diisopropylphenyl derivative **3b** ($\lambda = 538$ nm), along with a slightly higher overall extinction coefficient of 56200 $M^{-1}cm^{-1}$.

Accordingly, also the almost identical fluorescence spectra revealed emission maxima for both investigated dicarboximides at $\lambda = 572$ nm with only small Stokes shift of 1140 cm^{-1}. The fluorescence quantum yield of **3a** ($\Phi_{Fl} = 43\%$) is only slightly lower than for **3b** ($\Phi_{Fl} = 48\%$). Despite the varying imide substituents, the shapes and positions of the absorption as well as the fluorescence spectra are similar in the monomeric, non-aggregated state.

2.3. Self-Assembly Behavior

Because the bowl-to-bowl inversion was considered to hamper self-assembly of naphthalimide-annulated corannulene derivatives, we investigated this process by temperature-dependent ^{1}H-NMR spectroscopy in deuterated 1,1,2,2-tetrachloroethane (TCE-d_2).[17] Molecule **3a** is, however, not suitable for this kind of investigation due to the fast rotation of the phenyl rings attached to the imide units on the NMR time scale, making its protons indistuinguishable. In contrast, due to the two different faces (convex, concave) of the corannulene derivative and the steric hindrance of the diisopropylphenyl groups in molecule **3b**, the isopropyl groups attached at the phenyl ring in *ortho* position and the protons in *meta* position have different

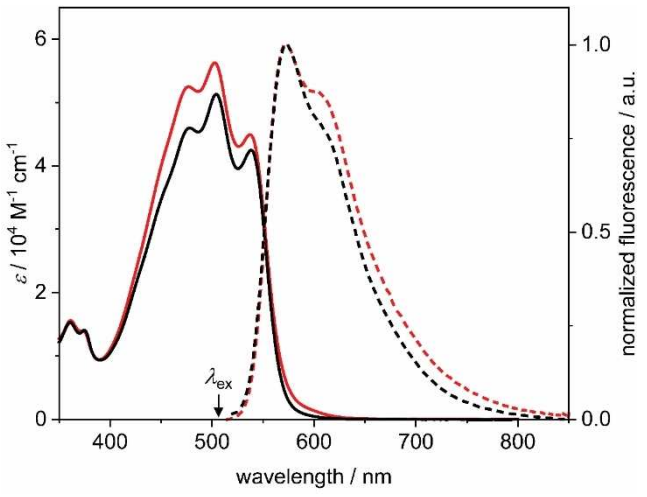

Figure 1. UV/Vis absorption (solid line) and fluorescence (dashed line, $\lambda_{ex} = 501$ nm) spectra of **3a** (red) and **3b** (black) in dichloromethane ($c = 1\cdot10^{-5}$ M, 25 °C).

chemical environments and can therefore be distuinguished at room temperature (Figure S5). Temperature-dependent ^{1}H-NMR studies revealed a coalescence temperature $T_c = 370$ K. At temperatures above this temperature the bowl-to-bowl interconversion is very fast and thus the signals are not distinguishable anymore.It is possible to calculate the rate constant of the inversion at the coalescence temperature as $k = 65.2\ s^{-1}$ and the free energy of activation to be $\Delta G^{\neq} = 78.4\ kJ\,mol^{-1}$, which is in good accordance with the value obtained by theoretical calculations (B3LYP/def2svp) of $\Delta G = 76.6\ kJ\,mol^{-1}$ (Figure S6). These values indicate the slow bowl-to-bowl interconversion of naphthalimide-annulated corannulene at room temperature, which should accordingly not disturb the self-assembly.

At room temperature, the signals of **3b** appear quite sharp in TCE-d_2, indicating the lack of aggregation due to the sterically demanding diisopropyl groups (Figure S5). In contrast, in the absence of sterically demanding *ortho*-substituents, the aggregation of molecule **3a** can be observed utilizing temperature-dependent ^{1}H-NMR spectroscopic investigations in the high-boiling solvent TCE-d_2. At low temperatures, broad signals are observed in the aromatic region of the spectra, whereas upon the increase of the temperature a significant narrowing of the signals occurs and a downfield shift of the aromatic protons signals can be observed, which is attributed to the formation of the monomer (Figure S7). The aliphatic region of the spectra is also affected by the aggregation-dependent broadening of signals. Similar behavior is observed in temperature-dependent ^{1}H-NMR spectra of **3a** in toluene-d_8. In this low-polar aromatic solvent, the change towards sharp signals is monitored at higher temperatures than in TCE-d_2, indicating the higher thermodynamic driving force for the formation of aggregates (Figure S8), which is in accordance with common observations of other dye aggregates like perylene bisimides (PBIs)[28] and phthalocyanines.[29]

Deeper insights into the formation of aggregates was obtained by concentration-dependent UV/Vis spectroscopy in toluene due to the low polarity of the solvent and the good solubility up to 150 mg mL^{-1} of **3a** in this solvent, which is one order of magnitude higher than the solubility of **3b** (Figure 2A).

Upon increasing the concentration of **3a** a pronounced broadening of the absorption band and a loss of its structure is detectable, suggesting distinct intermolecular interactions between the chromophores. Clear isosbestic points at 410 nm and 555 nm can be observed which indicate the existence of an equilibrium between the monomer and an aggregated species. The data could be fitted with the anti-cooperative K_2-K aggregation model[30] with a nucleus size of 2, giving $K_2 = 2.4 \cdot 10^4\ M^{-1}$ and a cooperativity factor $\sigma = 58$ (see Figure S11). Accordingly, the initial dimerization is highly favoured over the elongation ($K = 4.1 \cdot 10^2\ M^{-1}$) and the elongation constants are

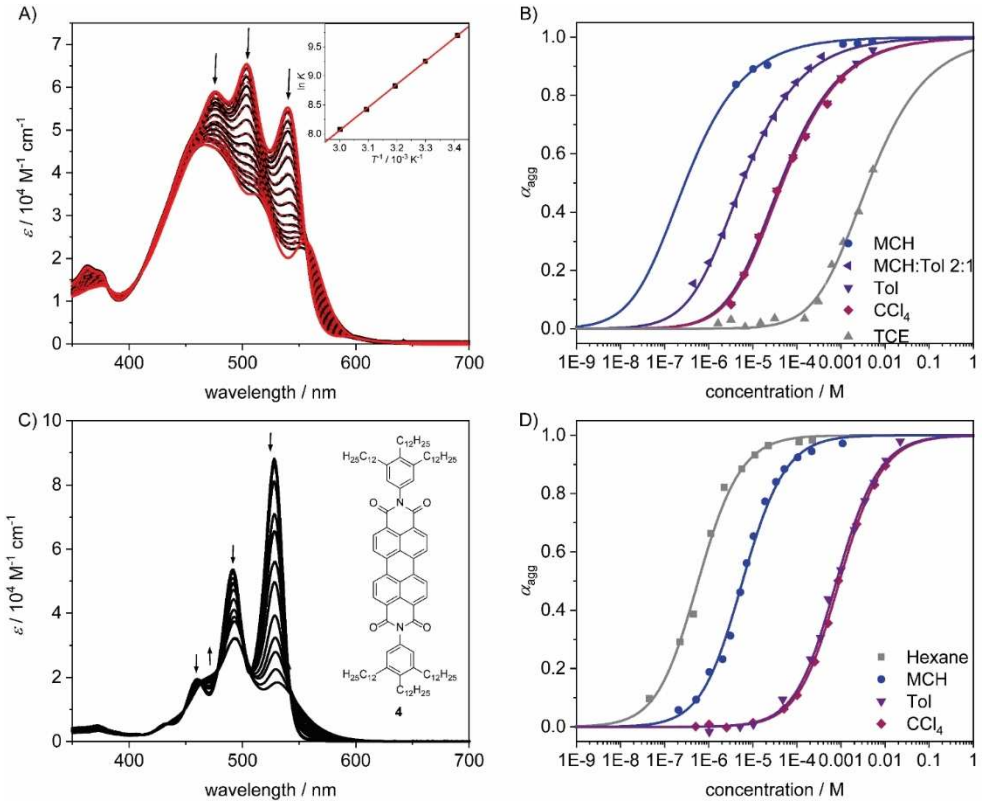

Figure 2. Concentration-dependent UV/Vis spectra at 25 °C of A) **3a** (black, $c = 4.5 \cdot 10^{-7}$–$4.0 \cdot 10^{-3}$ M) in toluene, the global fit analysis according to the monomer-dimer model for **3a** (red, dashed lines) and the ideal monomer and dimer spectra (red solid lines). Inset: Van't Hoff plot for the calculation of the thermodynamic parameters; B) Molar fraction of aggregated molecules α_{agg} as a function of concentration of **3a** fitted with the dimer model; C) Concentration-dependent UV/Vis spectra of PBI **4** in toluene ($c = 1.0 \cdot 10^{-6}$–$2.2 \cdot 10^{-2}$ M) and D) molar fraction of aggregated molecules (α_{agg}) as a function of concentration of **4** fitted with the isodesmic model. Reproduced from Ref. [28] with permission from The Royal Society of Chemistry.

prone to significant errors because only small amounts of the dimers further aggregate under the given experimental conditions. For this reason, the more simple monomer-dimer[29] model also afforded a good fit of the experimental data and was therefore applied for the following solvent-dependent aggregation studies. The dimerization constant K_D, that is obtained by application of this model in toluene, is $2.4 \cdot 10^4$ M^{-1}, which is in perfect accordance with the nucleation constant obtained by the anti-cooperative model. The resulting Gibbs energy change ΔG^0 was calculated to be -24.5 kJ mol^{-1} and the ideal monomer and dimer spectra were obtained as well (Figure 2A).

Similar spectral changes from the monomeric to the dimeric species could be observed by a decrease of the temperature of a solution of **3a** in toluene (Figure S9a). The thermodynamic parameters could be determined by performing concentration-dependent UV/Vis measurements at five different temperatures in toluene with the help of a van't Hoff plot to be $\Delta H^0 = -33.1$ kJ mol^{-1}, $\Delta S^0 = -10.8$ J K^{-1} and $\Delta G^0 = -23.6$ kJ mol^{-1}. The value for the Gibbs energy change obtained from this analysis is comparable to the one obtained from the dimerization constant at room temperature. The negative enthalpy and entropy reveal an enthalpy-driven self-assembly process for **3a** in toluene.

Additional concentration-dependent investigations have been conducted in solvents of different polarity to assess the aggregation behavior and strength in dependence of the different environments. For this purpose, unpolar methylcyclohexane (MCH), a mixture of MCH and toluene in a ratio of 2:1, tetrachloromethane and 1,1,2,2-tetrachloroethane (TCE) have been chosen. All spectral data could be fitted with the monomer-dimer model as well as with the anti-cooperative model (Figure S10). Due to the above mentioned reasons, the values obtained by the monomer-dimer model are discussed in the following paragraph. For the lowest (MCH) and highest (TCE) polar solvents, the values obtained by the fitting routine represent an approximation due to too strong (MCH) or rather weak (TCE) dimerization, respectively. As all the other data can be fitted according to the monomer-dimer model, it is reasonable to presume comparable aggregation behavior in MCH and TCE as well. The obtained values for the dimerization constant K_D are summarized in Table 2 and depicted as a function of the molar fraction of aggregated molecules in dependence of the concentration in Figure 2B. K_D is, as expected, highly solvent-dependent, varying from the lowest value of $2.4 \cdot 10^2$ M^{-1} in polar TCE to a four orders in magnitude higher value $3 \cdot 10^6$ M^{-1} in the low polarity solvent MCH.

To the best of our knowledge, this is the first report of aggregation constants for corannulene derivatives in solution. The herein obtained values are comparable to the values reported for phthalocyanine dimers ($K_D = 3.0 \cdot 10^6$ M^{-1}) in CCl_4,[31] extended PBI aggregates ($K = 1.5 \cdot 10^7$ M^{-1}) in MCH[32] and merocyanine dimers ($K_D = 2.1 \cdot 10^7 M^{-1}$) in CCl_4.[33] As these systems exhibit the highest aggregation constants reported so far, the new corannulene derivative is among the strongest self-assembling motifs, when decorated with proper substituents.

As bay-unsubstituted PBI dyes are congeners of the investigated corannulene derivative **3a**, a comparison to the well-studied PBI **4**, with the same solubilizing chains, might help to predict the properties of other new derivatives. Similar trends for the self-assembly should be observed for both molecules in different solvents, thus future optimization of the side chain for even higher aggregation constants might be performed analogous to PBI molecules.[28] A loss of the structure of the absorption band and its broadening upon aggregation is found for **3a** in a solution of toluene as well as for PBI **4** (Figure 2C). The comparison of the aggregation constants K of molecule **3a** and the congener PBI **4**, shows a significant increase by approximately two orders of magnitude for **3a** in the three solvents, which were investigated for both molecules, MCH, toluene and CCl_4 (Table 2).[28] This shows the extraordinary high tendency of the new class of corannulene derivatives bearing brush-like imide residues to self-assemble, which seem not to hinder the aggregation by their steric demand.

2.4. Structural Elucidation

The changes in the emission spectra of dye **3a** (Figure 3) are also of high interest for the characterization of the aggregate and a comparison to PBI **4**. Depending on the concentration, the color of the emitted light changes from yellow ($c = 1 \cdot 10^{-7}$ M) via orange to red ($c = 2 \cdot 10^{-3}$ M). A similar change of the color depending on the fraction of aggregated molecules in solution and the emission band is observed for the congener **4** in MCH.[32] Upon aggregation, a broad, structureless emission band, that is attributed to the dimer, emerges at 550 nm to 850 nm, which is also very similar to the excimer emission of PBI **4**.[34,35] The fluorescence quantum yield (Φ_{FI}) of **3a** in toluene is even higher (54%) than the already substantial quantum yield of the monomer in DCM (43%, Table 1). Remarkably, the

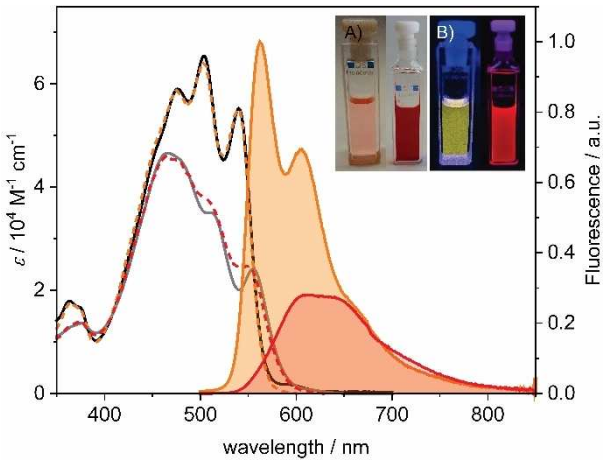

Figure 3. UV/Vis absorption spectra (monomer: black; dimer: grey) of **3a** in toluene at 25 °C and the respective fluorescence (solid lines; $\lambda_{ex} = 469$ nm) as well as excitation (dashed lines) spectra of monomer (orange, $c = 1 \cdot 10^{-7}$ M; $\lambda_{em} = 605$ nm) and dimer (red, $c = 2 \cdot 10^{-3}$ M; $\lambda_{em} = 650$ nm). The inset shows the optical photographs of the sample solutions under A) ambient and B) black light illumination.

Table 1. Optical properties of corannulene derivatives **3a** and **3b** as well as PBI **4**[a] in dichloromethane and toluene at 25 °C.

	Solvent	λ_{abs} [nm]	ε [$M^{-1}cm^{-1}$]	λ_{em} [nm]	Φ_{Fl} [%]	τ [ns]	Stokes shift [cm^{-1}]
3a	DCM	536, 503, 477	52500, 56200, 44900	572	43[b]	4.92	1140
3a (M)	Toluene	540, 504, 477	55250, 65400, 59000	562	54[c]	4.32	730
3a (D)	Toluene	555, 466	24100, 46600	612	24[c]	8.56 (89%) 2.81 (11%)	1680
3b	DCM	538, 504, 478	45900, 51300, 42500	573	48[b]	5.00	1140
4[26]	DCM	527, 491, 460	96300, 58100, 21000	532	63	3.2	180

[a] For molecular structure of PBI **4**, see Figure 2C. [b] Fluorescence quantum yields were determined relative to a standard dye (*N,N'*-bis(2,6-diisopropylphenyl)-3,4,9,10-perylenetetracarboxylic diimide.[27] [c] Fluorescence quantum yields were determined with an integrating sphere and corrected for reabsorption.

Table 2. Comparison of the dimerization constant K_D of **3a** and the isodesmic aggregation constant K of PBI **4** in different solvents at 25 °C.

	K_D (**3a**) [M^{-1}]	K (**4**) [M^{-1}][c]
Hexane	–[a]	$1.2\cdot10^6$
MCH	$\sim3\cdot10^6$[b]	$9.7\cdot10^4$
MCH/Toluene 2:1	$1.8\cdot10^5$	–
Toluene	$2.4\cdot10^4$	$5.9\cdot10^2$
CCl_4	$2.1\cdot10^4$	$6.5\cdot10^2$
TCE	$2.4\cdot10^2$	–

[a] Insufficient solubility at room temperature; [b] the value could only be estimated due to the small change in the absorption band even at the most diluted conditions; [c] Taken from Ref. [28]; MCH = methylcyclohexane, TCE = 1,1,2,2-tetrachloroethane.

aggregate also exhibits a quite high quantum yield of 24% despite of the contortion of the π-scaffold that is known to favour intersystem crossing.[36] Time-resolved measurements indicated a significant increase of the lifetime from $\tau = 4.32$ ns for the monomer to 8.56 ns for the dimer. Similar as for PBI **4**,[34,35] the longer lifetime is characteristic for a partially forbidden radiative process, presumably from an excimer-like excited state. This view is also corroborated by the absorption spectra of dimer **3a** which show a decrease of the intensity of the 0,0 transition and a hypsochromic shift of the absorption maximum compared to the monomer which are indicative for a H-type exciton coupling.[37,38]

Supporting evidence for the formation of dimers has been obtained by AFM measurements that were performed by spin coating solutions of different concentrations of **3a** in toluene (monomeric: $c = 2\cdot10^{-5}$ M and aggregated: $c = 3\cdot10^{-3}$ M) onto TPA-modified SiO_2/AlO_x substrates (Figure 4). Spin-coating leads

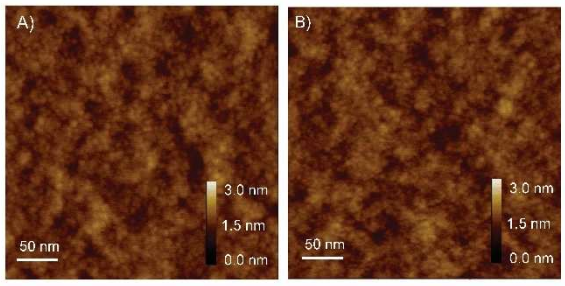

Figure 4. AFM height images of **3a** prepared by spin-coating onto TPA-modified SiO_2/AlO_x substrates from toluene at a concentration of A) $c = 2\cdot10^{-5}$ M ($\alpha_{agg} = 0.11$) and B) $c = 3\cdot10^{-3}$ M ($\alpha_{agg} = 0.91$).

to the formation of a multi-layered film consisting of small spherical particles with the height of 0.5–0.9 nm for the diluted sample, which is in accordance with the height found for **3b** in the crystal structure[24] and 0.5–1.0 nm of the concentrated sample, respectively. The height values indicate the presence of species of similar size in the order of the individual molecules in both solutions. Obviously, the AFM images do not indicate the formation of any larger-sized columnar aggregates which were observed for PBI **4** and other related PBI aggregates whose self-assembly is characterized by an isodesmic growth.[34] Accordingly, the preferentially dimerized **3a** species in solution obviously do not form defined extended aggregates upon solvent evaporation during the spin-coating process.

To further confirm the presence of dimers of **3a** in solution, DOSY NMR studies were performed in TCE-d_2 ($c = 5\cdot10^{-3}$ M) at 260 K as well as 390 K, where either mostly dimers ($\alpha_{agg} = 0.9$) or monomers ($\alpha_{agg} = 0.1$) are present. The diffusion coefficients of $D_M = 4.19\cdot10^{-10}$ m^2s^{-1} for the monomeric species at elevated temperatures and $D_D = 4.31\cdot10^{-11}$ m^2s^{-1} for the dimeric species at low temperatures have been determined. The hydrodynamic radii of both species were obtained by solving the Stokes-Einstein equation using the inherent solvent as standard, giving $r_M = 13.7$ Å for the monomer and $r_D = 15.6$ Å for the dimer, respectively (Figure S11). The obtained values match the dimension of a dimer at high concentrations and room temperature in solution. Furthermore, the two obtained radii are very similar, and thus in agreement with the AFM measurements which revealed similar sized particles for the monomer and the aggregate on TPA-modified surfaces.

To gain further insight into the precise arrangement of the molecules within the dimers, semi-empirical calculations (PM6-D3H4) were performed. Geometry optimizations for the dimer of **3a** afforded two structures of lowest energy, driven either primarily by the maximization of π-overlap (dispersion interactions) or the antiparallel alignment of the ground state dipole moments (electrostatic interactions). The maximization of π-π-interactions between the concave and convex face of the corannulene derivative is realized in the structure shown in Figure 5A, making the system overall 11 kJ mol^{-1} lower in energy compared to the structure in Figure 5B. The structural motif in Figure 5A also resembles the one calculated for corannulenes without appended naphthalimide units which suggested the formation of eclipsed dimers to be energetically favoured.[39]

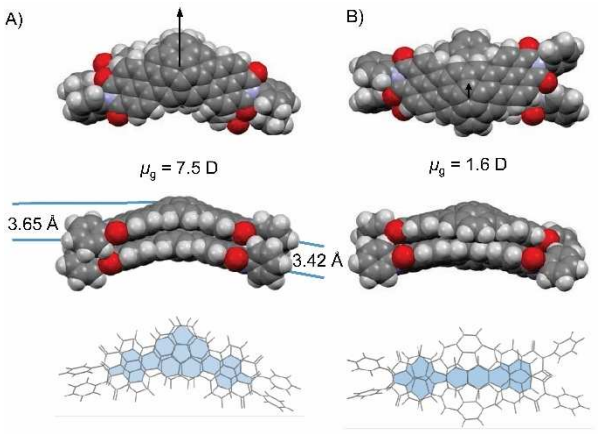

Figure 5. Top and side views onto two geometry-optimized (PM6-D3H4) structures that are lowest in energy for the dimer of **3a** governed either by A) intimate π-π-stacking or B) electrostatic dipole-dipole interactions. Bottom: Comparison of the minimal overlap of the π-systems (light blue area) of both dimeric structures of **3a**. The dodecyl chains were omitted for the geometry optimization.

In this favoured structure, depicted in Figure 5A, two corannulene moieties stack on top of each other in a parallel fashion. As a consequence, the overall ground state dipole moments sum up to $\mu_g = 7.5$ D compared to the monomeric species ($\mu_g = 3.8$ D). Previous theoretical investigations of corannulene dimers showed that the interactions between these curved π-systems are of comparable magnitude to those of similarly sized planar systems.[39] In these studies an equilibrium distance between two bowl-shaped corannulene molecules of 3.6 Å has been determined. In contrast, the equilibrium distance between two planarized corannulene moieties has been calculated to be 3.4 Å, which is similar to the π-π-distance in PBI molecules.[39]

Both values can be found in our new system, as the distance between the two bowls is calculated to be 3.65 Å in average, whereas the distance between the planar naphthalene moieties is about 3.42 Å. In our opinion, this minor distortion of the π-scaffold to enable a closer contact between neighboring naphthalimide units is the reason for the increase of the dimerization constant and the concomitant decrease of the elongation constant for this molecule. Similar observations have been made for PBIs which self-assemble with equal *K*-values for the two π-faces (i.e. isodesmic) as long as they are planar[34] but prefer to only dimerize after distortion by substituents in the bay area.[40] Another minor influence could be given by sterical congestions between the side chains that are located rather close in space due to the small rotational displacements for the lower energy dimer structure displayed in Figure 5A. Notably, this rotational displacement is by far smaller than for perylene bisimides.[34]

In contrast, in the second structure shown in Figure 5B, the dimerization is strongly governed by the antiparallel alignment of the two corannulene moieties, almost completely cancelling the ground state dipole moment to $\mu_g = 1.6$ D. In this structure, less overlap of the two π-systems is observed. Both structures are quite similar in size and energy, thus it is not possible to differentiate them in solution by the applied experimental techniques.

3. Conclusions

In conclusion, we have studied the self-assembly of a new naphthalimide-annulated corannulene derivative, with tridodecylphenyl substituents to obtain high solubility even in low polar solvents such as MCH. The ability to form supramolecular dimers of outstanding thermodynamic stability in solution in the investigated concentration range was confirmed by UV/Vis, ^{1}H and DOSY NMR spectroscopy as well as AFM. To the best of our knowledge, this is the first report on the self-assembly of a corannulene derivative in solution. The dimerization constants of up to $> 10^6$ M^{-1} in MCH are among the highest ones reported for π-conjugated systems, being in the same order of magnitude as those reported for phthalocyanine dimers ($K_D = 3.0 \cdot 10^6$ M^{-1}) in CCl_4, extended PBI aggregates ($K = 1.5 \cdot 10^7$ M^{-1}) in MCH and merocyanine dimers ($K_D = 2.1 \cdot 10^7$ M^{-1}) in CCl_4. Direct comparison to a structurally related PBI congener demonstrated the high propensity of our naphthalimide-annulated corannulene to self-assemble in a variety of solvents. The small size of the aggregates has been confirmed by AFM and DOSY measurements. By taking into account the different forces (dispersion, electrostatics) participating in the dimerization, we were able to propose two optimized structures for the aggregate by semi-empirical calculations, one showing parallel alignment driven by π-π-interactions and the other antiparallel alignment, supported by dipolar interactions. Having a significantly higher degree of π-overlap and a by 11 kJ mol^{-1} higher stability, the likelihood for the prevalence of the parallel structure is higher. Further variations of the naphthalimide-annulated corannulene motif might provide a variety of new self-assembled supramolecular structures in solution. Such aggregates may also enable applications of these bowl-shaped molecules as electron accepting materials in organic solar cells and photodetector devices in combination with p-type semiconducting polymers.[41,42]

Experimental Section

Materials & Methods

Reagents were purchased from commercial suppliers and used as received without further purification. Dichloromethane and ethylacetate were distilled prior to use. All reactions were carried out under nitrogen atmosphere. Column chromatography was performed with commercial glass columns using silica gel 60 M (particle size 0.04–0.063 mm; Merck KGaA) as stationary phase. Size-exclusion chromatography was performed on BioBeads S-X1 using HPLC grade solvents. NMR spectra were recorded on a Bruker *Avance III HD 400* or *Avance III HD 600* spectrometer and are calibrated to the residual proton signal of the used deuterated solvent. The chemical shifts (δ) are reported in parts per million (ppm) and coupling constants *J* in Hertz (Hz). Multiplicities for proton signals are abbreviated as s, d and m for singlet, doublet

and multiplet, respectively. MALDI-TOF mass spectra were recorded with an *autoflex II* mass spectrometer (Bruker Daltonics GmbH) using DCBT (2-[(2*E*)-3-(4-*tert*-butylphenyl)-2-methylprop-2-enylidene]malononitrile) as matrix. High resolution mass spectra (ESI) were recorded with an *ESI micrOTOF Focus* mass spectrometer (Bruker Daltronics GmbH). UV/Vis absorption spectra were recorded on a *JASCO V-770* or *Perkin-Elmer Lambda 950* spectrometer and fluorescence spectra on a *FLS980* fluorescence spectrometer (Edinburgh Instruments). Absolute quantum yields were determined on a Hamamatsu Absolute PL Quantum Yield Measurement System *CC9920-02*. AFM measurements were performed using a Bruker *Multimode 8 SPM* system operating in tapping mode. The samples were prepared by spin-coating toluene solutions of the molecule **3 a** onto TPA-functionalized SiO_2/AlO_x-substrates. Theoretical calculations were performed by Gaussian 09 program using DFT B3LYP/def2svp or the semi-empirical PM6-D3H4 method[43,44] as implemented in MOPAC2016.[45] Optimized ground-state geometries were examined by frequency analysis to possess no negative frequency.

4-Bromo-5-chloronaphthalene-1,8-dicarboxylic anhydride[24] and 3,4,5-tridodecylaniline[26] were synthesized according to procedures reported in the literature. Molecule **3 b** was resynthesized according to the literature.[24]

Synthesis of 2 a

4-Bromo-5-chloronaphthalene-1,8-dicarboxylic anhydride (8.68 mg, 27.9 μmol), 3,4,5-tridodecylaniline (50 mg, 83.6 μmol) and acetic acid (1 mL) were charged in a flask. The reaction mixture was stirred at 110 °C for 16h. After cooling, the product was obtained by silica gel column chromatography (cyclohexane: dichloromethane 9:1) to give **2 a** (4.3 mg, 4.82 μmol, 17 %) as a slightly orange solid. Mp. 34°C. ^{1}H-NMR (400 MHz, $CDCl_3$): δ [ppm] = 8.56 (d, J = 8.0 Hz, 1H), 8.44 (d, J = 8.0 Hz, 1H), 8.21 (d, J = 8.0 Hz, 1H), 7.94 (d, J = 8.0 Hz, 1H), 6.91 (s, 2H), 2.63 (m, 6H), 1.39–1.25 (m, 60 H), 0.87 (t, J = 7 Hz, 9H); ^{13}C-NMR (100 MHz, $CDCl_3$): δ *[ppm]* = 163.5, 163.3, 142.2, 139.4, 139.2, 136.1, 131.87, 131.80, 131.74, 131.67, 127.3, 127.1, 126.9, 126.0, 123.3, 122.8, 33.1, 31.93, 31.90, 31.2, 30.7, 30.39, 30.37, 29.9, 29.73, 29.71, 29.68, 29.67, 29.66, 29.64, 29.59, 29.5, 29.4, 29.38, 29.35, 28.8, 22.70, 22.68, 14.12, 14.11; MS (MALDI-TOF, pos. mode, DCTB in $CHCl_3$): m/z calculated for $C_{54}H_{81}BrClNO_2^+$ $[M+H]^+$: 890.52, found: 890.54; HRMS (DIP-MS, pos. mode): *m/z* calculated for $C_{54}H_{82}BrClNO_2^+$ $[M]^+$: 890.5212, found: 890.5208.

Synthesis of 3 a

Corannulene diboronic acid bis(pinacol)ester **1** (100 mg, 199 μmol), precursor **2 a** (223 mg, 440 μmol), tris(dibenzylideneacetone) dipalladium(0)-chloroform adduct (10.4 mg, 10.0 μmol), tri(*m*-tolyl) phosphine (12.2 mg, 40.0 μmol), caesium carbonate (391 mg, 1.20 mmol) and 1-chloronaphthalene (6 mL) were placed in a Schlenk tube. The reaction mixture was stirred at 100 °C for 1d. After cooling to room temperature, cyclohexane was added and the mixture was purified by column chromatography using ethyl acetate as eluent followed by DCM. Size-exclusion chromatography on BioBeads S-X1 (DCM:MeOH 9:1) gave **3 a** as a dark red solid (100mg, 55.6 μmol, 28 %). Mp. 330 °C. ^{1}H-NMR (400 MHz, TCE-d_2, 390 K): δ [ppm] = 8.68 (d, J = 7.9 Hz, 2H), 8.65 (d, J = 7.9 Hz, 2H), 8.49 (d, J = 7.9 Hz, 2H), 8.43 (d, J = 7.9 Hz, 2H), 8.32 (s, 2H), 8.24 (s, 2H), 7.81 (s, 2H), 6.94 (s, 4H), 2.67 (m, 12H), 1.66–1.62 (m, 12H), 1.45–1.25 (m, 108H), 0.90–0.86 (m, 18H); ^{13}C-NMR (100 MHz, TCE-d_2, 390 K): δ[ppm] = 162.8, 162.7, 141.3, 138.4, 136.8, 136.0, 135.8, 133.0 132.4, 132.2, 132.1, 132.0, 130.5, 130.0, 129.5, 128.2, 127.9, 126.7, 126.3, 122.7, 122.52, 122.47, 121.2, 32.6, 31.3, 31.2, 30.6, 29.9, 29.4, 29.07, 29.04, 28.98, 28.88, 28.65, 28.62; 21.9; MS (MALDI-TOF, neg. mode, DCTB in $CHCl_3$): *m/z* calculated for $C_{128}H_{168}N_2O_4^-$ $[M]^-$: 1797.301, found: 1797.298; HRMS (ESI-TOF, pos. mode, acetonitrile/chloroform 1/1) *m/z*: calculated for $C_{128}H_{168}N_2NaO_4^+$: 1820.2896 $[M+Na]^+$, found: 1820.2807; UV/Vis ($c = 1 \cdot 10^{-5}$ M, DCM, 293 K): $\varepsilon_{max}(\lambda_{max}) =$ 56200 $M^{-1}cm^{-1}$ (503 nm); Fluorescence (DCM): λ_{max} (λ_{ex}) = 572 nm (501 nm); $\Phi = 0.43 \pm 0.04$.

Acknowledgements

We are grateful for financial support from the Deutsche Forschungsgemeinschaft (Grant Wu 317/20-1). This publication was funded by the German Research Foundation (DFG) and the University of Würzburg in the funding programme Open Access Publishing. We thank Joachim O. Lindner (Würzburg) for the theoretical calculations, Chia-An Shen (Würzburg) for the AFM measurements and Dr. Kazutaka Shoyama (Würzburg) for his advice for the synthesis.

Conflict of Interest

The authors declare no conflict of interest.

Keywords: corannulene · π-π-interactions · self-assembly · aggregation · supramolecular chemistry

[1] F. J. Lovas, R. J. McMahon, J. U. Grabow, M. Schnell, J. Mack, L. T. Scott, R. L. Kuczkowski, *J. Am. Chem. Soc.* **2005**, *127*, 4345–4349.
[2] E. M. Muzammil, D. Halilovic, M. C. Stuparu, *Commun. Chem.* **2019**, *2*, 58.
[3] J. Guilleme, E. Cavero, T. Sierra, J. Ortega, C. L. Folcia, J. Etxebarria, T. Torres, D. Gonzalez-Rodriguez, *Adv. Mater.* **2015**, *27*, 4280–4284.
[4] C. G. Claessens, D. Gonzalez-Rodriguez, B. del Rey, T. Torres, G. Mark, H. P. Schuchmann, C. von Sonntag, J. G. MacDonald, R. S. Nohr , *Eur. J. Org. Chem.* **2003**, *14*, 2547–2551.
[5] M. Saito, H. Shinokubo, H. Sakurai, *Mater. Chem. Front.* **2018**, *2*, 635–661.
[6] J. M. Lehn, *PNAS* **2002**, *99*, 4763–4768.
[7] J. M. Lehn, *Science* **2002**, *295*, 2400–2403.
[8] S. Sreejith, N. V. Menon, Y. Wang, H. Joshi, S. Liu, K. C. Chong, Y. Kang, H. Sun, M. C. Stuparu, *Mater. Chem. Front.* **2017**, *1*, 831–837.
[9] K. Shoyama, F. Würthner, *J. Am. Chem. Soc.* **2019**, *141*, 13008–13012.
[10] K. Kawasumi, Q. Y. Zhang, Y. Segawa, L. T. Scott, K. Itami, *Nat. Chem.* **2013**, *5*, 739–744.
[11] J. M. Fernandez-Garcia, P. J. Evans, S. Medina Rivero, I. Fernandez, D. Garcia-Fresnadillo, J. Perles, J. Casado, N. Martin, *J. Am. Chem. Soc.* **2018**, *140*, 17188–17196.
[12] L. N. Dawe, T. A. AlHujran, H. A. Tran, J. I. Mercer, E. A. Jackson, L. T. Scott, P. E. Georghiou, *Chem. Commun.* **2012**, *48*, 5563–5565.
[13] S. Mizyed, P. E. Georghiou, M. Bancu, B. Cuadra, A. K. Rai, P. Cheng, L. T. Scott, *J. Am. Chem. Soc.* **2001**, *123*, 12770–12774.
[14] A. Sygula, F. R. Fronczek, R. Sygula, P. W. Rabideau, M. M. Olmstead, *J. Am. Chem. Soc.* **2007**, *129*, 3842–3843.
[15] Y.-Y. Xu, H.-R. Tian, S.-H. Li, Z.-C. Chen, Y.-R. Yao, S.-S. Wang, X. Zhang, Z.-Z. Zhu, S.-L. Deng, Q. Zhang, S. Yang, S.-Y. Xie, R.-B. Huang, L.-S. Zheng, *Nat. Commun.* **2019**, *10*, 485.
[16] W. Sun, Y. Wang, L. Ma, L. Zheng, W. Fang, X. Chen, H. Jiang, *J. Org. Chem.* **2018**, *83*, 14667–14675.
[17] K. Yoshida, A. Osuka, *Chem. Eur. J.* **2015**, *21*, 11727–11734.
[18] J. Guilleme, J. Arago, E. Orti, E. Cavero, T. Sierra, J. Ortega, C. L. Folcia, J. Etxebarria, D. Gonzalez-Rodriguez, T. Torres, *J. Mater. Chem. C* **2015**, *3*, 985–989.
[19] M. A. Petrukhina, *Dalton Trans.* **2019**, *48*, 5125–5130.
[20] S. N. Spisak, A. V. Zabula, A. S. Filatov, A. Y. Rogachev, M. A. Petrukhina, *Angew. Chem. Int. Ed.* **2011**, *50*, 8090–8094; *Angew. Chem.* **2011**, *123*, 8240–8244.

[21] A. Haupt, D. Lentz, *Chem. Eur. J.* **2018**, *25*, 3440–3454.
[22] A. Haupt, R. Walter, B. Loll, D. Lentz, *Eur. J. Org. Chem.* **2018**, 6338–6342.
[23] D. Meng, G. Liu, C. Xiao, Y. Shi, L. Zhang, L. Jiang, K. K. Baldridge, Y. Li, J. S. Siegel, Z. Wang, *J. Am. Chem. Soc.* **2019**, *141*, 5402–5408.
[24] K. Shoyama, D. Schmidt, M. Mahl, F. Würthner, *Org. Lett.* **2017**, *19*, 5328–5331.
[25] K. Shoyama, M. Mahl, S. Seifert, F. Würthner, *J. Org. Chem.* **2018**, *83*, 5339–5346.
[26] F. Würthner, Z. J. Chen, V. Dehm, V. Stepanenko, *Chem. Commun.* **2006**, 1188–1190.
[27] F. Fennel, J. Gershberg, M. Stolte, F. Würthner, *Phys. Chem. Chem. Phys.* **2018**, *20*, 7612–7620.
[28] Z. J. Chen, B. Fimmel, F. Würthner, *Org. Biomol. Chem.* **2012**, *10*, 5845–5855.
[29] Z. J. Chen, A. Lohr, C. R. Saha-Möller, F. Würthner, *Chem. Soc. Rev.* **2009**, *38*, 564–584.
[30] J. Gershberg, F. Fennel, T. H. Rehm, S. Lochbrunner, F. Würthner, *Chem. Sci.* **2016**, *7*, 1729–1737.
[31] A. R. Monahan, A. F. Deluca, J. A. Brado, *J. Phys. Chem.* **1972**, *76*, 446–449.
[32] F. Würthner, C. Thalacker, S. Diele, C. Tschierske, *Chem. Eur. J.* **2001**, *7*, 2245–2253.
[33] F. Würthner, S. Yao, T. Debaerdemaeker, R. Wortmann, *J. Am. Chem. Soc.* **2002**, *124*, 9431–9447.
[34] Z. Chen, V. Stepanenko, V. Dehm, P. Prins, L. D. A. Siebbeles, J. Seibt, P. Marquetand, V. Engel, F. Würthner, *Chem. Eur. J.* **2007**, *13*, 436–449.
[35] J. M. Lim, P. Kim, M. C. Yoon, J. Sung, V. Dehm, Z. Chen, F. Würthner, D. Kim, *Chem. Sci.* **2013**, *4*, 388–397.
[36] K. Nagarajan, A. R. Mallia, K. Muraleedharan, M. Hariharan, *Chem. Sci.* **2017**, *8*, 1776–1782.
[37] F. C. Spano, *Acc. Chem. Res.* **2010**, *43*, 429–439.
[38] T. Brixner, R. Hildner, J. Köhler, C. Lambert, F. Würthner, *Adv. Energy Mater.* **2017**, *7*, 1700236.
[39] A. Sygula, S. Saebø, *Int. J. Quantum Chem.* **2009**, *109*, 65–72.
[40] Z. Chen, U. Baumeister, C. Tschierske, F. Würthner, *Chem. Eur. J.* **2007**, *13*, 450–465.
[41] A. Nowak-Król, K. Shoyama, M. Stolte, F. Würthner, *Chem. Commun.* **2018**, *54*, 13763–13772.
[42] Y. Zhong, T. J. Sisto, B. Zhang, K. Miyata, X.-Y. Zhu, M. L. Steigerwald, F. Ng, C. Nuckolls, *J. Am. Chem. Soc.* **2017**, *139*, 5644–5647.
[43] J. J. P. Stewart, *J. Mol. Model.* **2007**, *13*, 1173–1213.
[44] J. Řezáč, P. Hobza *J. Chem. Theory Comput.* **2012**, *8*, 141–151.
[45] MOPAC2016, Version: 16.230 L, James J. P. Stewart, *Stewart Computational Chemistry*, Colorado Springs, CO, USA, web: HTTP://OpenMOPAC.net (**2016**).

Manuscript received: September 25, 2019